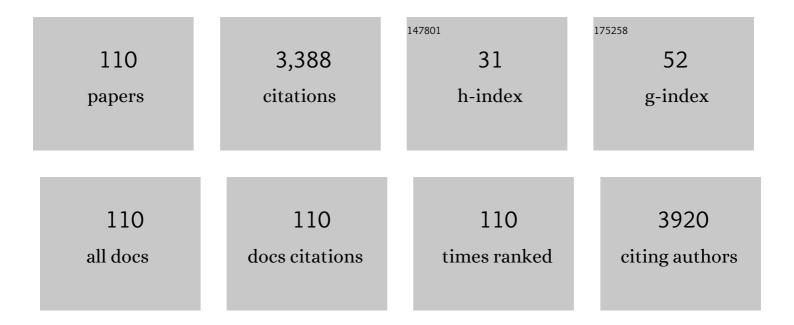
Kaspars Tars

List of Publications by Year in descending order

Source: https://exaly.com/author-pdf/1639532/publications.pdf Version: 2024-02-01



#	Article	IF	CITATIONS
1	Rapid Proton-Detected NMR Assignment for Proteins with Fast Magic Angle Spinning. Journal of the American Chemical Society, 2014, 136, 12489-12497.	13.7	254
2	Structure of fully protonated proteins by proton-detected magic-angle spinning NMR. Proceedings of the United States of America, 2016, 113, 9187-9192.	7.1	224
3	Sulfocoumarins (1,2-Benzoxathiine-2,2-dioxides): A Class of Potent and Isoform-Selective Inhibitors of Tumor-Associated Carbonic Anhydrases. Journal of Medicinal Chemistry, 2013, 56, 293-300.	6.4	199
4	Efficient Expression and Crystallization System of Cancer-Associated Carbonic Anhydrase Isoform IX. Journal of Medicinal Chemistry, 2015, 58, 9004-9009.	6.4	141
5	NMR Spectroscopic Assignment of Backbone and Sideâ€Chain Protons in Fully Protonated Proteins: Microcrystals, Sedimented Assemblies, and Amyloid Fibrils. Angewandte Chemie - International Edition, 2016, 55, 15504-15509.	13.8	116
6	Asymmetric cryo-EM reconstruction of phage MS2 reveals genome structure in situ. Nature Communications, 2016, 7, 12524.	12.8	114
7	New anticancer drug candidates sulfonamides as selective hCA IX or hCA XII inhibitors. Bioorganic Chemistry, 2018, 77, 411-419.	4.1	99
8	Long-chain acylcarnitines determine ischaemia/reperfusion-induced damage in heart mitochondria. Biochemical Journal, 2016, 473, 1191-1202.	3.7	77
9	The crystal structure of bacteriophage GA and a comparison of bacteriophages belonging to the major groups of Escherichia coli leviviruses. Journal of Molecular Biology, 1997, 271, 759-773.	4.2	75
10	Structure and Function of CutC Choline Lyase from Human Microbiota Bacterium Klebsiella pneumoniae. Journal of Biological Chemistry, 2015, 290, 21732-21740.	3.4	70
11	X-ray crystallography-promoted drug design of carbonic anhydrase inhibitors. Chemical Communications, 2015, 51, 7108-7111.	4.1	61
12	Dynamic Nuclear Polarizationâ€Enhanced Biomolecular NMR Spectroscopy at High Magnetic Field with Fast Magicâ€Angle Spinning. Angewandte Chemie - International Edition, 2018, 57, 7458-7462.	13.8	56
13	Fragment-Based Discovery of 2-Aminoquinazolin-4(3 <i>H</i>)-ones As Novel Class Nonpeptidomimetic Inhibitors of the Plasmepsins I, II, and IV. Journal of Medicinal Chemistry, 2016, 59, 374-387.	6.4	55
14	Out-and-back 13C–13C scalar transfers in protein resonance assignment by proton-detected solid-state NMR under ultra-fast MAS. Journal of Biomolecular NMR, 2013, 56, 379-386.	2.8	54
15	The True Story and Advantages of RNA Phage Capsids as Nanotools. Intervirology, 2016, 59, 74-110.	2.8	52
16	The Three-Dimensional Structure of Bacteriophage PP7 from Pseudomonas aeruginosa at 3.7-Ã Resolution. Virology, 2000, 272, 331-337.	2.4	49
17	Highly efficient production of phosphorylated hepatitis B core particles in yeast Pichia pastoris. Protein Expression and Purification, 2011, 75, 218-224.	1.3	48
18	Structural Basis of RNA Binding Discrimination between Bacteriophages QÎ ² and MS2. Structure, 2006, 14, 487-495	3.3	47

#	Article	IF	CITATIONS
19	Plasmepsin Inhibitory Activity and Structure-Guided Optimization of a Potent Hydroxyethylamine-Based Antimalarial Hit. ACS Medicinal Chemistry Letters, 2014, 5, 373-377.	2.8	46
20	Structure of AP205 Coat Protein Reveals Circular Permutation in ssRNA Bacteriophages. Journal of Molecular Biology, 2016, 428, 4267-4279.	4.2	45
21	ls protein deuteration beneficial for proton detected solid-state NMR at and above 100ÂkHz magic-angle spinning?. Solid State Nuclear Magnetic Resonance, 2017, 87, 126-136.	2.3	45
22	Encapsulation mechanisms and structural studies of GRM2 bacterial microcompartment particles. Nature Communications, 2020, 11, 388.	12.8	44
23	Targeting Carnitine Biosynthesis: Discovery of New Inhibitors against Î ³ -Butyrobetaine Hydroxylase. Journal of Medicinal Chemistry, 2014, 57, 2213-2236.	6.4	41
24	3 <i>H</i> -1,2-benzoxathiepine 2,2-dioxides: a new class of isoform-selective carbonic anhydrase inhibitors. Journal of Enzyme Inhibition and Medicinal Chemistry, 2017, 32, 767-775.	5.2	41
25	N -Substituted and ring opened saccharin derivatives selectively inhibit transmembrane, tumor-associated carbonic anhydrases IX and XII. Bioorganic and Medicinal Chemistry, 2017, 25, 3583-3589.	3.0	39
26	Structural Basis for Featuring of Steroid Isomerase Activity in Alpha Class Glutathione Transferases. Journal of Molecular Biology, 2010, 397, 332-340.	4.2	38
27	The three-dimensional structure of cocksfoot mottle virus at 2.7 å resolution. Virology, 2003, 310, 287-297.	2.4	36
28	Structural Basis of the Suppressed Catalytic Activity of Wild-type Human Glutathione Transferase T1-1 Compared to its W234R Mutant. Journal of Molecular Biology, 2006, 355, 96-105.	4.2	36
29	Potent SARS-CoV-2 mRNA Cap Methyltransferase Inhibitors by Bioisosteric Replacement of Methionine in SAM Cosubstrate. ACS Medicinal Chemistry Letters, 2021, 12, 1102-1107.	2.8	36
30	Investigating the structural basis of purine specificity in the structures of MS2 coat protein RNA translational operator hairpins. Nucleic Acids Research, 2002, 30, 2678-2685.	14.5	34
31	New Substituted Piperazines as Ligands for Melanocortin Receptors. Correlation to the X-ray Structure of "THIQ― Journal of Medicinal Chemistry, 2004, 47, 4613-4626.	6.4	32
32	Vaccination against IL-31 for the treatment of atopic dermatitis in dogs. Journal of Allergy and Clinical Immunology, 2018, 142, 279-281.e1.	2.9	32
33	Eliminating Factor H-Binding Activity of Borrelia burgdorferi CspZ Combined with Virus-Like Particle Conjugation Enhances Its Efficacy as a Lyme Disease Vaccine. Frontiers in Immunology, 2018, 9, 181.	4.8	32
34	5-Substituted-(1,2,3-triazol-4-yl)thiophene-2-sulfonamides strongly inhibit human carbonic anhydrases I, II, IX and XII: Solution and X-ray crystallographic studies. Bioorganic and Medicinal Chemistry, 2013, 21, 5130-5138.	3.0	31
35	Crystal structure of human gamma-butyrobetaine hydroxylase. Biochemical and Biophysical Research Communications, 2010, 398, 634-639.	2.1	30
36	Diversity of pili-specific bacteriophages: genome sequence of IncM plasmid-dependent RNA phage M. BMC Microbiology, 2012, 12, 277.	3.3	30

#	Article	IF	CITATIONS
37	Alternative mutations of a positively selected residue elicit gain or loss of functionalities in enzyme evolution. Proceedings of the National Academy of Sciences of the United States of America, 2006, 103, 4876-4881.	7.1	29
38	Crystal Structure of the Bacteriophage QÎ ² Coat Protein in Complex with the RNA Operator of the Replicase Gene. Journal of Molecular Biology, 2014, 426, 1039-1049.	4.2	29
39	The three-dimensional structure of ryegrass mottle virus at 2.9ÂÃ resolution. Virology, 2007, 369, 364-374.	2.4	28
40	<i>N</i> -Acylbenzenesulfonamide Dihydro-1,3,4-oxadiazole Hybrids: Seeking Selectivity toward Carbonic Anhydrase Isoforms. ACS Medicinal Chemistry Letters, 2017, 8, 792-796.	2.8	27
41	The Structure of Bacteriophage φCb5 Reveals a Role of the RNA Genome and Metal Ions in Particle Stability and Assembly. Journal of Molecular Biology, 2009, 391, 635-647.	4.2	26
42	Production and purification of chimeric HBc virus-like particles carrying influenza virus LAH domain as vaccine candidates. BMC Biotechnology, 2017, 17, 79.	3.3	26
43	Novel fluorinated carbonic anhydrase IX inhibitors reduce hypoxia-induced acidification and clonogenic survival of cancer cells. Oncotarget, 2018, 9, 26800-26816.	1.8	25
44	AP205 VLPs Based on Dimerized Capsid Proteins Accommodate RBM Domain of SARS-CoV-2 and Serve as an Attractive Vaccine Candidate. Vaccines, 2021, 9, 403.	4.4	25
45	Structural Analysis of a Glutathione Transferase A1-1 Mutant Tailored for High Catalytic Efficiency with Toxic Alkenals. Biochemistry, 2009, 48, 7698-7704.	2.5	24
46	Crystal structure of the readâ€ŧhrough domain from bacteriophage Qβ A1 protein. Protein Science, 2011, 20, 1707-1712.	7.6	24
47	Crystal structures of the Erp protein family members ErpP and ErpC from Borrelia burgdorferi reveal the reason for different affinities for complement regulator factor H. Biochimica Et Biophysica Acta - Proteins and Proteomics, 2015, 1854, 349-355.	2.3	24
48	Crystal Structure of the Maturation Protein from Bacteriophage QÎ ² . Journal of Molecular Biology, 2017, 429, 688-696.	4.2	24
49	Genome Structure of Caulobacter Phage phiCb5. Journal of Virology, 2011, 85, 4628-4631.	3.4	21
50	The Capsid of the Small RNA Phage PRR1 Is Stabilized by Metal Ions. Journal of Molecular Biology, 2008, 383, 914-922.	4.2	20
51	5-Substituted-benzylsulfanyl-thiophene-2-sulfonamides with effective carbonic anhydrase inhibitory activity: Solution and crystallographic investigations. Bioorganic and Medicinal Chemistry, 2017, 25, 857-863.	3.0	20
52	Structural characterization of CspZ, a complement regulator factor <scp>H</scp> and <scp>FHL</scp> â€1 binding protein from <i><scp>B</scp>orreliaÂburgdorferi</i> . FEBS Journal, 2014, 281, 2613-2622.	4.7	19
53	Structure of Phage fr Capsids with a Deletion in the FG Loop: Implications for Viral Assembly. Virology, 1998, 249, 80-88.	2.4	18
54	Structure and stability of icosahedral particles of a covalent coat protein dimer of bacteriophage MS2. Protein Science, 2009, 18, 1653-1661.	7.6	18

#	Article	IF	CITATIONS
55	Complete Genome Sequence of the Enterobacter cancerogenus Bacteriophage Enc34. Journal of Virology, 2012, 86, 11403-11404.	3.4	18
56	Zuordnung der Rückgrat―und Seitenkettenâ€Protonen in vollstädig protonierten Proteinen durch Festkörperâ€NMRâ€&pektroskopie: Mikrokristalle, Sedimente und Amyloidfibrillen. Angewandte Chemie, 2016, 128, 15730-15735.	2.0	18
57	Molecular basis for regulation of Src by the docking protein p130Cas. Journal of Molecular Recognition, 2006, 19, 30-38.	2.1	17
58	Crystal packing of a bacteriophage MS2 coat protein mutant corresponds to octahedral particles. Protein Science, 2008, 17, 1731-1739.	7.6	17
59	Structure-Based Redesign of GST A2-2 for Enhanced Catalytic Efficiency with Azathioprine. Chemistry and Biology, 2012, 19, 414-421.	6.0	17
60	Synthesis of novel dipeptide sulfonamide conjugates with effective carbonic anhydrase I, II, IX, and XII inhibitory properties. Bioorganic Chemistry, 2018, 81, 311-318.	4.1	17
61	Structural and functional analysis of BB0689 from Borrelia burgdorferi , a member of the bacterial CAP superfamily. Journal of Structural Biology, 2015, 192, 320-330.	2.8	16
62	Modulating Catalytic Activity by Unnatural Amino Acid Residues in a GSH-Binding Loop of GST P1-1. Journal of Molecular Biology, 2008, 376, 811-826.	4.2	15
63	Structural Basis for DNA Recognition of a Single-stranded DNA-binding Protein from Enterobacter Phage Enc34. Scientific Reports, 2017, 7, 15529.	3.3	15
64	Structure determination of bacteriophage PP7 fromPseudomonas aeruginosa: from poor data to a good map. Acta Crystallographica Section D: Biological Crystallography, 2000, 56, 398-405.	2.5	14
65	Expression and purification of active, stabilized trimethyllysine hydroxylase. Protein Expression and Purification, 2014, 104, 1-6.	1.3	14
66	Structures of plasmepsin II from <i>Plasmodium falciparum</i> in complex with two hydroxyethylamine-based inhibitors. Acta Crystallographica Section F, Structural Biology Communications, 2015, 71, 1531-1539.	0.8	14
67	Structure of an outer surface lipoprotein BBA64 from the Lyme disease agent <i>Borrelia burgdorferi</i> which is critical to ensure infection after a tick bite. Acta Crystallographica Section D: Biological Crystallography, 2013, 69, 1099-1107.	2.5	13
68	The Factor H-Binding Site of CspZ as a Protective Target against Multistrain, Tick-Transmitted Lyme Disease. Infection and Immunity, 2020, 88, .	2.2	13
69	Different Binding Modes of Free and Carrier-Protein-Coupled Nicotine in a Human Monoclonal Antibody. Journal of Molecular Biology, 2012, 415, 118-127.	4.2	12
70	PRR1 coat protein binding to its RNA translational operator. Acta Crystallographica Section D: Biological Crystallography, 2013, 69, 367-372.	2.5	12
71	Production and characterization of novel ssRNA bacteriophage virus-like particles from metagenomic sequencing data. Journal of Nanobiotechnology, 2019, 17, 61.	9.1	12
72	Human carnitine biosynthesis proceeds via (2S,3S)-3-hydroxy-N ^ε -trimethyllysine. Chemical Communications, 2017, 53, 440-442.	4.1	11

#	Article	IF	CITATIONS
73	Target highlights from the first postâ€PSI CASP experiment (CASP12, May–August 2016). Proteins: Structure, Function and Bioinformatics, 2018, 86, 27-50.	2.6	11
74	Construction and Immunogenicity of a Novel Multivalent Vaccine Prototype Based on Conserved Influenza Virus Antigens. Vaccines, 2020, 8, 197.	4.4	11
75	Structural Analysis of an Antigen Chemically Coupled on Virusâ€Like Particles in Vaccine Formulation. Angewandte Chemie - International Edition, 2021, 60, 12847-12851.	13.8	11
76	Structural characterization of the Borrelia burgdorferi outer surface protein BBA73 implicates dimerization as a functional mechanism. Biochemical and Biophysical Research Communications, 2013, 434, 848-853.	2.1	10
77	Yeast-Expressed Bacteriophage-Like Particles for the Packaging of Nanomaterials. Molecular Biotechnology, 2014, 56, 102-110.	2.4	10
78	2-Aminoquinazolin-4(3H)-one based plasmepsin inhibitors with improved hydrophilicity and selectivity. Bioorganic and Medicinal Chemistry, 2018, 26, 2488-2500.	3.0	10
79	CntA oxygenase substrate profile comparison and oxygen dependency of TMA production in <i>Providencia rettgeri</i> . Journal of Basic Microbiology, 2018, 58, 52-59.	3.3	10
80	Structure and applications of novel influenza HA tri-stalk protein for evaluation of HA stem-specific immunity. PLoS ONE, 2018, 13, e0204776.	2.5	10
81	Protein-RNA Interactions in the Single-Stranded RNA Bacteriophages. Sub-Cellular Biochemistry, 2018, 88, 281-303.	2.4	10
82	Halogenated and di-substituted benzenesulfonamides as selective inhibitors of carbonic anhydrase isoforms. European Journal of Medicinal Chemistry, 2020, 185, 111825.	5.5	10
83	Assembly of mixed rod-like and spherical particles from group I and II RNA bacteriophage coat proteins. Virology, 2009, 391, 187-194.	2.4	9
84	Crystal structure of the infectious phenotype-associated outer surface protein BBA66 from the Lyme disease agent Borrelia burgdorferi. Ticks and Tick-borne Diseases, 2014, 5, 63-68.	2.7	9
85	Dynamic Nuclear Polarizationâ€Enhanced Biomolecular NMR Spectroscopy at High Magnetic Field with Fast Magicâ€Angle Spinning. Angewandte Chemie, 2018, 130, 7580-7584.	2.0	8
86	Structural analysis of the outer surface proteins from Borrelia burgdorferi paralogous gene family 54 that are thought to be the key players in the pathogenesis of Lyme disease. Journal of Structural Biology, 2020, 210, 107490.	2.8	8
87	Crystal structure of Borrelia burgdorferi outer surface protein BBA69 in comparison to the paralogous protein CspA. Ticks and Tick-borne Diseases, 2019, 10, 1135-1141.	2.7	7
88	BBE31 from the Lyme disease agent Borrelia burgdorferi, known to play an important role in successful colonization of the mammalian host, shows the ability to bind glutathione. Biochimica Et Biophysica Acta - General Subjects, 2020, 1864, 129499.	2.4	7
89	Diversity of the lysozyme fold: structure of the catalytic domain from an unusual endolysin encoded by phage Enc34. Scientific Reports, 2022, 12, 5005.	3.3	7
90	QSAR of multiple mutated antibodies. Journal of Molecular Recognition, 2007, 20, 97-102.	2.1	6

#	Article	IF	CITATIONS
91	Extending the Inhibition Profiles of Coumarin-Based Compounds Against Human Carbonic Anhydrases: Synthesis, Biological, and In Silico Evaluation. Molecules, 2019, 24, 3580.	3.8	6
92	Novel ssRNA phage VLP platform for displaying foreign epitopes by genetic fusion. Vaccine, 2020, 38, 6019-6026.	3.8	6
93	Three-dimensional structure of 22 uncultured ssRNA bacteriophages: Flexibility of the coat protein fold and variations in particle shapes. Science Advances, 2020, 6, .	10.3	6
94	Variety of size and form of GRM2 bacterial microcompartment particles. Protein Science, 2021, 30, 1035-1043.	7.6	6
95	Nâ€Terminal Modification of Glyâ€Hisâ€Tagged Proteins with Azidogluconolactone. ChemBioChem, 2021, 22, 3199-3207.	2.6	6
96	Isoform-Selective Enzyme Inhibitors by Exploring Pocket Size According to the Lock-and-Key Principle. Biophysical Journal, 2020, 119, 1513-1524.	0.5	6
97	Methyl 2-Halo-4-Substituted-5-Sulfamoyl-Benzoates as High Affinity and Selective Inhibitors of Carbonic Anhydrase IX. International Journal of Molecular Sciences, 2022, 23, 130.	4.1	6
98	Crystal structure of the membrane attack complex assembly inhibitor BGA71 from the Lyme disease agent Borrelia bavariensis. Scientific Reports, 2018, 8, 11286.	3.3	5
99	Aryl-4,5-dihydro-1H-pyrazole-1-carboxamide Derivatives Bearing a Sulfonamide Moiety Show Single-digit Nanomolar-to-Subnanomolar Inhibition Constants against the Tumor-associated Human Carbonic Anhydrases IX and XII. International Journal of Molecular Sciences, 2020, 21, 2621.	4.1	5
100	Crystal structure of <i>Plasmodium falciparum</i> proplasmepsin IV: the plasticity of proplasmepsins. Acta Crystallographica Section F, Structural Biology Communications, 2016, 72, 659-666.	0.8	4
101	Structural analysis of BorreliaÂburgdorferi periplasmic lipoprotein BB 0365 involved in Lyme disease infection. FEBS Letters, 2020, 594, 317-326.	2.8	4
102	Crystal structure of the N-terminal domain of the major virulence factor BB0323 from the Lyme disease agent <i>Borrelia burgdorferi</i> . Acta Crystallographica Section D: Structural Biology, 2019, 75, 825-830.	2.3	3
103	ssRNA Phages: Life Cycle, Structure and Applications. , 2020, , 261-292.		3
104	Solution <scp>NMR</scp> structure of <i>Borrelia burgdorferi</i> outer surface lipoprotein <scp>BBP28</scp> , a member of the <i>mlp</i> protein family. Proteins: Structure, Function and Bioinformatics, 2021, 89, 588-594.	2.6	3
105	Sample Preparation Induced Artifacts in Cryo-Electron Tomographs. Microscopy and Microanalysis, 2012, 18, 1043-1048.	0.4	2
106	Plasmid dimerization increases the production of hepatitis B core particles in E. coli. Biotechnology and Bioprocess Engineering, 2013, 18, 850-857.	2.6	2
107	X-Ray Crystallographic Structures of High-Affinity and High-Selectivity Inhibitor Complexes with CA IX That Plays a Special Role in Cancer. , 2019, , 203-213.		0
108	Structural and Functional Analysis of BBA03, Borrelia burgdorferi Competitive Advantage Promoting Outer Surface Lipoprotein. Pathogens, 2020, 9, 826.	2.8	0

#	Article	IF	CITATIONS
109	Struktur eines an virusänliche Partikel gekoppelten Antigens: Analyse einer Impfstoffâ€Formulierung. Angewandte Chemie, 2021, 133, 12957-12961.	2.0	Ο
110	A Positively Selected Residue Influences Enzyme Functionalities. FASEB Journal, 2006, 20, A474.	0.5	0